2023 Volume 8, Issue 2
Advances in Precision Medicine
ISSN: 2424-9106 (Online)
ISSN: 2424-8592 (Print)

Application and Mechanism of Renal Tubular Perilipin 2 in Predicting Decline in Renal Function in Diabetic Kidney Disease Patients

Rui Shen, Xin Yu, Caifeng Shi, Songyan Qin, Yi Fang, Aiqin He, Xiaomei Wu, Junwei Yang*, Yang Zhou*
Center for Kidney Disease, The Second Affiliated Hospital of Nanjing Medical University, Nanjing 210003, China

***Corresponding authors:** Yang Zhou, zhouyang@njmu.edu.cn; Junwei Yang, jwyang@njmu.edu.cn

Abstract

Objective: To investigate whether changes in the expression of perilipin 2 (PLIN2) in renal tubular epithelial cells can predict the decline in renal function in diabetic kidney disease (DKD) and to elucidate the mechanism by which PLIN2 promotes tubular epithelial cell damage in DKD. *Methods:* A retrospective cohort study was conducted involving 12 non-diabetic patients (as controls) and 51 DKD patients. Demographic data and laboratory test results were collected. A simplified linear mixed-effects model was used to calculate the estimated glomerular filtration rate (eGFR) slope. The relationship between PLIN2 and renal function decline in DKD patients was analyzed using Spearman correlation and generalized linear models. In vivo experiments employed BKS-db/db mice and streptozotocin-induced diabetic mouse models. In vitro experiments used primary renal tubular epithelial cells treated with glucose, transfected with PLIN2 siRNA, or overexpressing PLIN2 plasmids. Protein immunoblotting and immunofluorescence staining were used to detect PLIN2 expression. Oil Red O staining assessed lipid droplet accumulation and a real-time cellular metabolic analyzer measured mitochondrial oxygen consumption rate (OCR). *Results:* The expression level of PLIN2 in renal tubules was significantly elevated in DKD patients compared to controls. Over a follow-up period of 24 (12, 39) months, the eGFR slope in DKD patients was -7.42 (-19.77, -2.09) mL/(min·1.73 m²·year). The baseline percentage of PLIN2-positive area in renal tubules was significantly associated with changes in the eGFR slope during follow-up *hazard ratio* (*HR*) = 1.90, 95, suggesting the predictive value of tubular PLIN2 for renal function decline in DKD. Diabetic mouse models exhibited significantly increased lipid droplet accumulation and PLIN2 expression in renal tubules compared to controls. In vitro, glucose treatment induced lipid droplet accumulation and increased PLIN2 expression in renal tubular epithelial cells. PLIN2 knockdown significantly alleviated glucose-induced lipid droplet accumulation, while PLIN2 overexpression exacerbated it. The decline in mitochondrial OCR caused by glucose treatment was mitigated by PLIN2 knockdown, whereas PLIN2 overexpression directly reduced mitochondrial OCR. *Conclusion:* PLIN2 in renal tubules can predict renal function decline in DKD patients. PLIN2 inhibits mitochondrial oxidative respiration, promotes lipid droplet accumulation in renal tubular epithelial cells, and contributes to the progression of DKD.

Keywords

Diabetic kidney disease
Perilipin 2
Estimated glomerular filtration rate slope
Lipid droplet
Oxygen consumption rate

Online publication: December 22, 2023

1. Introduction

Diabetic kidney disease (DKD) has become the leading cause of chronic kidney disease (CKD) in China. However, clinical indicators for assessing the risk of renal function decline in DKD remain insufficient. Studies have demonstrated increased levels of perilipin 2 (PLIN2) in the urine of DKD patients [1] and in the renal tissue of diabetic mouse models [2,3]. Furthermore, PLIN2 may contribute to the rapid progression of DKD mediated by fatty acids [4]. Nevertheless, the role of PLIN2 in DKD remains unclear. This study employs a retrospective cohort design to investigate the role of tubular PLIN2 in predicting renal function decline in DKD and explores the mechanism by which PLIN2 regulates lipid droplet accumulation to promote DKD progression in diabetic and renal tubular epithelial cell models.

2. Materials and methods

2.1. Study subjects and protocol

2.2.1. Study population

The study protocol was approved by the Ethics Committee of the Second Affiliated Hospital of Nanjing Medical University (Approval No. 2019KY097). Written informed consent was obtained from all participants. The study selected patients with type 2 diabetes complicated by diabetic kidney disease (DKD) who had undergone renal biopsies. Non-diabetic patients were included as the control group. Each participant had at least three recorded estimated glomerular filtration rate (eGFR) measurements during the follow-up period, with a minimum interval of three months between each measurement. Exclusion criteria included immune-related kidney disease, acute kidney injury, malignant tumors, previous renal replacement therapy, and severe diseases in other organs.

DKD was diagnosed based on renal pathology in accordance with the diagnostic criteria for type 2 diabetes established by the American Diabetes Association in 2020 [5].

Baseline data collected included height, weight, blood, and urine samples for biochemical analysis, as well as blood pressure and heart rate measurements taken in the clinic. Blood pressure and heart rate were measured three times at one-minute intervals, and the average value was used as the final measurement. eGFR was calculated using the Chronic Kidney Disease Epidemiology Collaboration (CKD-EPI) equation based on serum creatinine (http://www.nkdep.nih.gov). The eGFR slope [mL/(min·1.73m²·year)] during the follow-up period was calculated using a simplified linear mixed-effects model.

2.1.2. Diabetic mouse models

The animal experimental protocol was approved by the Ethics Committee of Nanjing Medical University. Spontaneous diabetes models were established using BKS-db/db mice (strain No. T002407, GemPharmatech), with db/m mice serving as controls. Mice were sacrificed at 16 weeks of age.

For streptozotocin (STZ)-induced diabetic models, 8-week-old C57BL/6J mice (Vital River) were used. A single dose of STZ (120 mg/kg) was administered via the tail vein. Mice with fasting blood glucose levels consistently above 16.7 mmol/L were considered diabetic. Mice were sacrificed in the 16th week after STZ injection, and kidney tissue samples were collected.

2.1.3. Primary renal tubular epithelial cell culture and treatment

Primary renal tubular epithelial cells were isolated using a collagenase digestion-density gradient centrifugation method [6]. Kidneys from 2- to 3-week-old mice were harvested, and the renal cortex was separated from the outer membrane and medulla. The cortex was minced and filtered through 80-, 100-, and 200-mesh stainless steel sieves. Renal tubules retained on the 200-mesh sieve were collected and digested with 0.25% trypsin to obtain high-density cell layers. Cells were cultured in DMEM/F12 medium containing 10% fetal bovine serum. Media were replaced after cell attachment, and cells were passaged 3–4 times to achieve morphological stability, followed by purity verification.

When cell confluence reached 80%, the medium

was replaced with a serum-free culture medium. Cells were treated with 30 mmol/L D-glucose, while control cells were treated with an equivalent concentration of D-mannitol to exclude the effect of glucose-induced hyperosmolarity. Cells were transfected with 50 nmol/L small interfering RNA (siRNA) or negative control (siNC), or with 1 μg/mL PLIN2-overexpressing plasmid (pPLIN2) or the empty vector pcDNA3.

2.2. Main reagents and instruments

PLIN2 antibody (15294-1-AP) was purchased from Proteintech; laminin antibody (ab44941) was purchased from Abcam; Oil Red O (O0625), STZ (S0130), D-glucose (G8270), and D-mannitol (M4125) were all purchased from Sigma-Aldrich; PLIN2 siRNA (siPLIN2; 5'-GGA UAA GAC CAA AGG AGC ATT-3', 5'-UGC UCC UUU GGU CUU AUC CTT-3'), siNC (5'-UUC UCC GAA CGU GUC ACG UTT-3', 5'-ACG UGA CAC GUU CGG AGA ATT-3'), pPLIN2, and pcDNA3 were all purchased from Nanjing Yike Biotechnology Co., Ltd.; Oligomycin (HY-N6782), carbonyl cyanide 4-(trifluoromethoxy) phenylhydrazone (FCCP; HY-100410), Antimycin A (HY-17559), and rotenone (HY-B1756) were purchased from MedChemExpress; Lipofectamine 3000 (L3000015) and Opti-MEM I reduced serum medium (11058021) were purchased from Invitrogen; Seahorse XF Pro cellular real-time metabolic analyzer was purchased from Agilent; P800 automated biochemical analyzer was purchased from Roche; Eclipse 80i microscope was purchased from Nikon.

2.3. Main experimental methods

2.3.1. Western blot

After renal cortical tissue or cells were lysed, protein samples of equal concentration were prepared. These samples were separated by polyacrylamide gel electrophoresis, transferred to a nitrocellulose membrane, and then blocked. The membrane was incubated with primary and secondary antibodies sequentially, and signal intensity was analyzed using ImageJ software.

2.3.2. Immunofluorescence staining

Renal cortical tissue or cells were sectioned into 3 μm thin slices, fixed, and blocked. Primary antibodies were added, followed by fluorescence-labeled secondary antibodies for incubation. Nuclei were stained with 4',6-diamidino-2-phenylindole (DAPI) and sealed. The samples were observed and photographed under a fluorescence microscope. The percentage of PLIN2-positive area within the renal tubules was analyzed in 10 fields per sample using ImageJ software.

2.3.3. Oil Red O staining

Renal cortical tissue or cells were sectioned into 10 μm slices, washed with 60% isopropanol, and stained with Oil Red O in the dark. After staining, samples were washed and stained with hematoxylin to visualize the nuclei, then sealed and observed under a microscope. The percentage of Oil Red O-positive area in 10 fields per sample was analyzed using ImageJ software.

2.3.4. Measurement of cellular oxygen consumption rate (OCR)

In Seahorse XF Pro cell culture plates, 1×10^5 cells were seeded per well. Baseline OCR was recorded, followed by the addition of 1 μmol/L oligomycin, 0.75 μmol/L FCCP, 1 μmol/L Antimycin A, and rotenone, and OCR was recorded after each addition. The total protein concentration of the cells was used to normalize the OCR data (unit: μmol/(min·g)).

2.4. Statistical analysis

Statistical analysis was performed using SPSS 25.0 and R software. Bartlett's test was used to determine the distribution characteristics of variables. Normally distributed continuous variables were expressed as mean ± standard deviation (SD), with comparisons between two groups conducted using the *t*-test and comparisons between multiple groups performed using analysis of variance (ANOVA). Non-normally distributed continuous variables were described as median (Q1, Q3), with comparisons between two groups performed using

the Mann-Whitney U test and comparisons between multiple groups using rank sum tests. Categorical variables were expressed as frequencies and percentages, with comparisons between groups conducted using the chi-square test. Spearman's correlation analysis and generalized linear models were used to predict the relationship between PLIN2 and renal function decline in DKD patients. A *P*-value of < 0.05 was considered statistically significant.

3. Results

3.1. General baseline characteristics of study subjects

The clinical characteristics of the DKD cohort are shown in **Table 1**. The median follow-up time was 24 (12, 39) months, with an eGFR slope of −7.42 (−19.77, −2.09) mL(/min·1.73 m²·year).

3.2. Increased expression of PLIN2 in renal tubules of DKD patients

Immunofluorescence staining showed that PLIN2 was predominantly located in the renal tubules. Compared with the control group, the percentage of PLIN2-positive area in the renal tubules of DKD patients was significantly higher ($P < 0.05$), as shown in **Figure 1**.

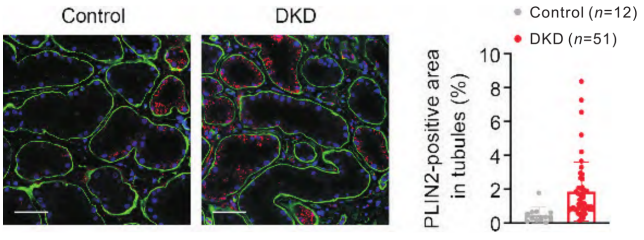

Figure 1. Expression or perilipin 2 (PLIN2) in kidney biopsy samples (immunofluorescence staining, scale bar = 50 μm). Red: PLIN2; Green: Laminin; Blue: DAPI. Mean ± SD. *P < 0.05 vs. control group

3.3. The percentage of PLIN2-positive area in renal tubules predicts renal function decline in DKD patients

As shown in **Table 2**, after adjusting for clinical characteristics such as eGFR, an increase in the percentage of PLIN2-positive area in the renal tubules at baseline was associated with a higher risk of an eGFR slope ≤ -5 mL/(min·1.73 m²·year) in DKD patients, with a hazard ratio (HR) of 1.90 [95% confidence interval (CI): 1.00–3.58]. The HR for patients with a higher percentage of PLIN2-positive area in the renal tubules at baseline (quantile 2 vs. quantile 1) was 4.08 (95% CI: 1.20–13.93), suggesting that PLIN2 in renal tubules can predict renal function decline in DKD patients.

Table 1. Characteristics of the study population at baseline

Characteristics	DKD (*n* = 51)
Age [year, median (Q_1, Q_3)]	57 (50, 64)
Female [*n* (%)]	15 (29.41)
Duration of diabetes [year, median (Q_1, Q_3)]	8 (3, 10)
Systolic blood pressure (mmHg, mean ± SD)	149.20 ± 21.14
Diastolic blood pressure [mmHg, median (Q_1, Q_3)]	85.00 (80.00, 91.00)
Fasting blood glucose [mmol/L, median (Q_1, Q_3)]	7.18 (5.82, 9.47)
HbAlc [%, median (Q_1, Q_3)]	7.40 (6.55, 8.30)
Total cholesterol [mmol/L. median (Q_1, Q_3)]	5.05 (3.89, 6.88)
Triglyceride [mmol/L, median (Q_1, Q_3)]	1.77 (1.13, 2.95)
eGFR [mL/(min·1.73 m²), median (Q_1, Q_3)]	55.76 (44.54, 80.88)

Table 2. Association of the baseline percentage of PLIN2-positive tubules with an eGFR slope ≤ -5 mL/(min·1.73 m²·year) in the DKD cohort at the 2-year follow-up

PLIN2-positive area in tubules (%)	DKD (*n* = 51)	
	HR (95% CI)	*P* value
1−SD increment	1.90 (1.00, 3.58)	0.048
Quartile 2 vs. quartile 1	4.08 (1.20, 13.93)	0.025

3.4. Accumulation of lipid droplets and increased expression of PLIN2 in renal tubules of diabetic mice and primary renal tubular epithelial cells treated with glucose

Oil Red O staining showed that lipid droplets accumulated in the renal tubules of db/db mice compared with db/m mice (**Figure 2A**). Immunofluorescence staining and Western blot results showed that the distribution and expression of PLIN2 were significantly increased in the renal tubules of db/db mice compared to db/m mice (**Figure 2B** and **C**). Similarly, in STZ-induced diabetic mice, lipid droplet accumulation (**Figure 2D**), as well as PLIN2 distribution (**Figure 2E**) and expression (**Figure 2F**), were significantly higher compared to control mice.

In primary renal tubular epithelial cells treated with glucose, a large number of lipid droplets appeared (**Figure 3A**), and PLIN2 showed a punctate distribution in the cytoplasm (**Figure 3B**). PLIN2 expression increased with the duration of glucose treatment (**Figure 3C**). These results suggest that diabetes leads to lipid droplet accumulation in renal tubular epithelial cells, accompanied by increased PLIN2 expression.

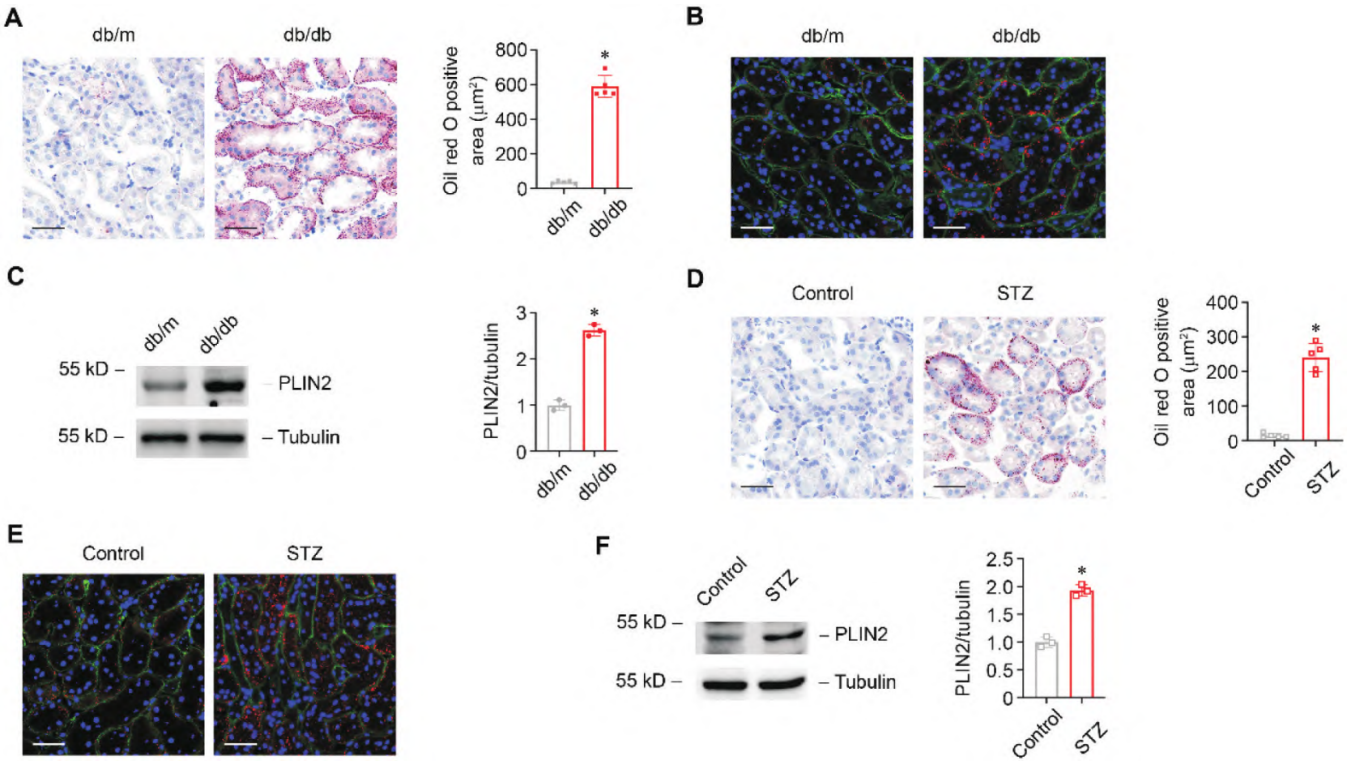

Figure 2. Accumulation of lipid droplets and expression of perilipin 2 (PLIN2) in the kidneys of diabetic mice. **(A)** Representative images of kidney sections from db/m and db/db mice assessed by oil red O staining (scale bar = 50 μm) and quantification of oil red O-positive area (*n* = 5); **(B)** Representative images of kidney sections from db/m and db/db mice assessed by immunofluorescence staining for PLIN2 (red: PLIN2; green: laminin; blue: DAPI; scale bar = 50 μm); **(C)** Western blot analysis of PLIN2 protein expression in the kidney cortex of db/m and db/db mice (*n* = 3); **(D)** Representative images of kidney sections from control and STZ-induced diabetic mice assessed by oil red O staining (scale bar = 50 μm) and quantification of oil red O-positive area (*n* = 5); **(E)** Representative images of kidney sections from control and STZ-induced diabetic mice assessed by immunofluorescence staining for PLIN2 (red: PLIN2; green laminin; blue: DAPI; scale bar = 50 μm); **(F)** Western blot analysis of PLIN2 protein expression in the kidney cortex of control and STZ-induced diabetic mice (*n* = 3). Mean ± SD. **P* < 0.05 vs db/m or control group

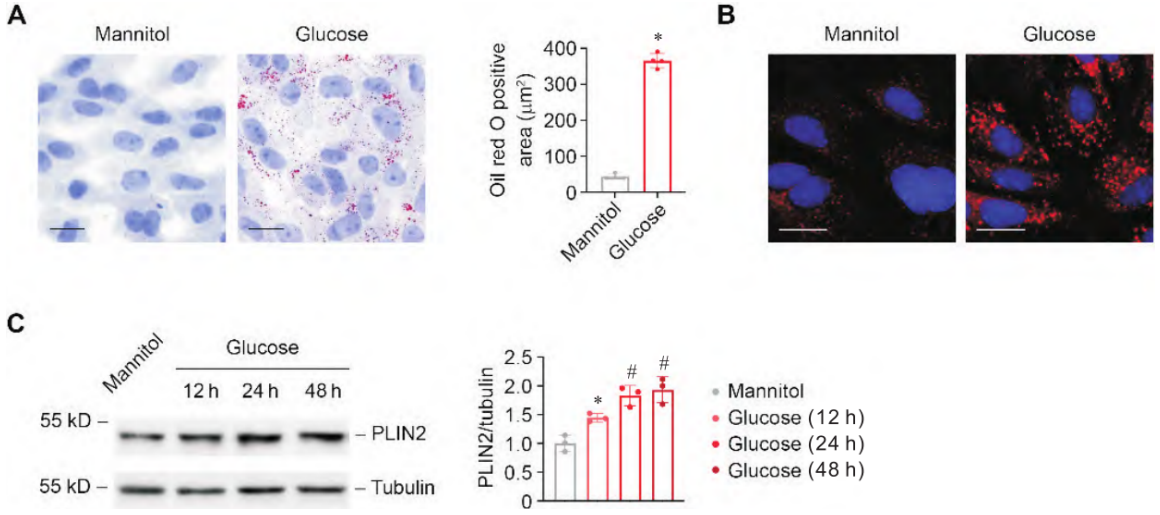

Figure 3. Accumulation of lipid droplets and expression of perilipin 2 (PLIN2) in glucose-treated renal tubular cells. **(A)** Representative images of control and glucose-treated renal tubular cells assessed by oil red O staining (scale bar = 10 μm) and quantification of oil red O-positive area (n = 4); **(B)** Representative images of control and glucose-treated renal tubular cells assessed by immunofluorescence staining for PLIN2 (red: PLIN2; blue: DAPI; scale bar = 10 μm); **(C)** Western blot analysis of PLIN2 protein expression in control and glucose-treated renal tubular cells (n = 3). Mean ± SD. *P < 0.05 vs mannitol group; #P < 0.05 vs glucose (12 h) group

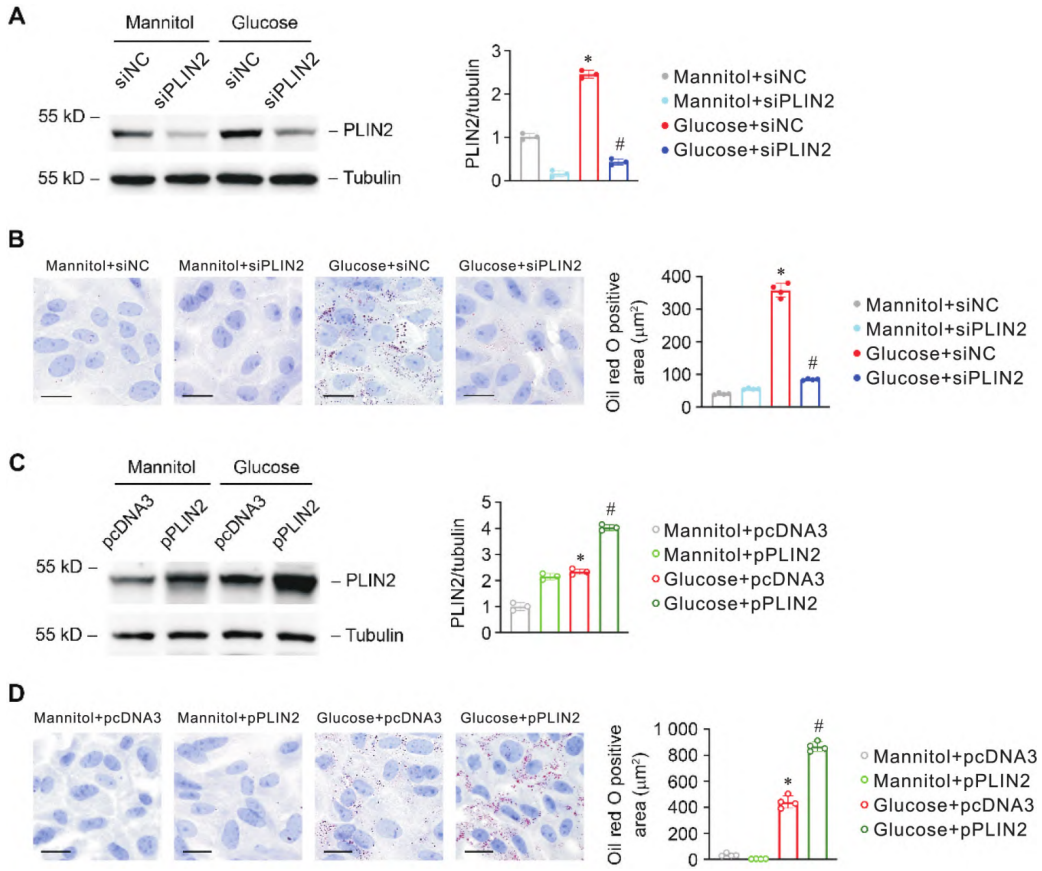

Figure 4. Perilipin 2 (PLIN2) regulated the accumulation of lipid droplets in glucose-treated renal tubular cells. **(A)** Western blot analysis of PLIN2 protein expression in control and glucose-treated renal tubular cells transfected with siNC or siPLIN2 (n = 3); **(B)** Representative images of control and glucose-treated renal tubular cells transfected with siNC or siPLIN2 (oil red O staining, scale bar = 10 μm) and quantification of oil red O-positive area (n = 4); **(C)** Western blot analysis of PLIN2 protein expression in control and glucose-treated renal tubular cells transfected with pcDNA3 or pPLIN2 (n = 3); **(D)** Representative images of control and glucose-treated renal tubular cells transfected with pcDNA3 or pPLIN2 (oil red O staining, scale bar = 10 μm) and quantification of oil red O-positive area (n = 4). Mean ± SD. *P < 0.05 vs mannitol + siNC group or mannitol + pcDNA3 group; #P < 0.05 vs glucose + siNC group or glucose + pcDNA3 group

3.5. PLIN2 regulates lipid droplet accumulation

After transfected with siRNA to knock down PLIN2 expression (**Figure 4A**), the accumulation of lipid droplets in glucose-treated cells was alleviated (**Figure 4B**). Conversely, after transfecting with a plasmid to overexpress PLIN2 (**Figure 4C**), the glucose-induced lipid droplet accumulation in cells was further aggravated (**Figure 4D**). This suggests that PLIN2 regulates lipid droplet accumulation in renal tubular epithelial cells.

3.6. PLIN2 regulates mitochondrial OCR in cells

OCR measurement results showed that after glucose treatment, the mitochondrial OCR in renal tubular epithelial cells (**Figure 5A**), including basal respiration, ATP production, maximal respiration, and spare respiratory capacity (**Figure 5B**), were significantly reduced compared to control cells. Transfection with siPLIN2 alleviated the impact of glucose on OCR. In contrast, transfection with the PLIN2-overexpressing plasmid directly decreased mitochondrial OCR in renal tubular epithelial cells (**Figure 5A**), including basal respiration, ATP production, maximal respiration, and spare respiratory capacity (**Figure 5B**). This suggests that PLIN2 regulates mitochondrial oxidative phosphorylation.

4. Discussion

4.1. The value of renal tubular PLIN2 in assessing DKD kidney injury and progression

DKD affects approximately 40% of diabetic patients, leading to kidney failure, cardiovascular diseases, and death [7]. Identifying high-risk populations for the progression of DKD has always been a challenging and prominent issue in clinical diagnosis and treatment [8]. Due to clinical phenotypic differences, such as proteinuria fluctuation or even normalization, rapid decline in GFR, and non-proteinuric DKD, the reliability of diagnosing and assessing DKD based on proteinuria and eGFR has been widely debated [9]. Studies have shown that demographic characteristics, lifestyle, biochemical data, and other factors are associated with DKD progression. Potential biomarkers, such as tumor necrosis factor receptors 1/2 [10,11], transforming growth factor β and bone morphogenetic protein 7 [12,13], matrix metalloproteinases 2/7/8/13 [14], and leucocyte methylation [15], have been identified. However, specific renal pathological changes, such as tubulointerstitial fibrosis and vascular sclerosis [16,17], are often directly related to kidney function decline in diabetic patients. Although DKD diagnosis does not rely on renal tissue biopsy, it is undeniable that renal pathological changes have a closer association with clinical progression compared to blood and urine markers. Evaluating the expression of PLIN2 in the renal tissue of DKD patients revealed its association with eGFR slopes during follow-up, suggesting that it can predict the progression of kidney function in DKD. Early detection of PLIN2 and intervention may benefit high-risk populations for DKD progression.

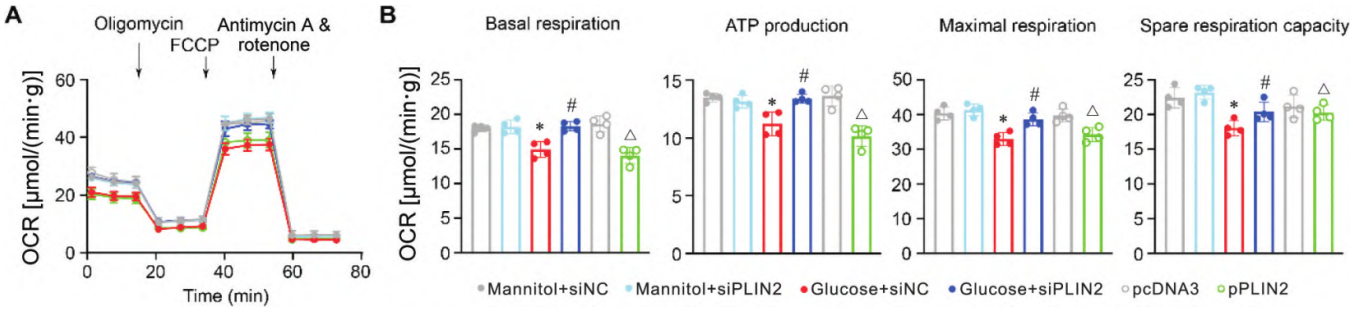

Figure 5. Perilipin 2 (PLIN2) regulated mitochondrial aerobic respiration in renal tubular cells. **(A)** representative traces showing the oxygen consumption rate (OCR) in renal tubular cells after various treatments as indicated; **(B)** Summary of the OCR data for renal tubular cells from 4 independent experiments. Mean ± SD. $n = 4$. *$P < 0.05$ vs mannitol + siNC group; $^{\#}P < 0.05$ vs glucose + siNC group; $^{\Delta}P < 0.05$ vs pcDNA3 group

4.2. The role of PLIN2 in regulating aerobic fatty acid metabolism in renal tubular epithelial cells in the progression of DKD

Almost all intrinsic renal cells and infiltrating inflammatory cells contribute to the progression of DKD [18]. However, recent studies suggest that GFR depends more on renal tubular cells than on glomerular cells [19], and the importance of renal tubules has been confirmed in both human and animal models [20]. Renal tubules significantly influence kidney hypertrophy and hyperperfusion, and their damage and loss are closely associated with eGFR decline and DKD progression [21]. Renal tubular epithelial cells contain abundant mitochondria and rely on fatty acid oxidation (FAO) within these mitochondria to efficiently produce energy and maintain physiological function. Abnormal FAO promotes cell injury [22], hinders cell repair [23], and is thus critical to the survival and function of renal tubules. Studies have indicated that lipid metabolism abnormalities are a central feature of kidney pathology [24], and are also common in DKD patients [21].

PLIN2 is one of the most well-known proteins in the family of lipid droplet-associated proteins, and it is the only member of this family with the broadest tissue distribution, particularly in renal tissue [25]. In the early stages of acute ischemic injury, a large accumulation of PLIN2-positive lipid droplets is present in renal tubules, but such accumulation is not observed in obstructive chronic kidney disease (CKD) models [26]. Phosphatidylcholine-mediated rapid progression of DKD involves the participation of peroxisome proliferator-activated receptor δ (PPARδ)-PLIN2 signaling [4]. PLIN2 is also associated with lipid accumulation in macrophages [27,28], and the infiltration of mononuclear macrophages expressing PLIN2 causes inflammation and capillary degeneration, which triggers diabetic retinopathy [29]. These findings suggest that PLIN2 is not simply a lipid droplet marker; its expression changes in diabetic renal tubules may directly participate in the progression of DKD. In this study, by intervening in the expression of PLIN2, its role in regulating lipid droplet accumulation in renal tubular epithelial cells induced by glucose was observed. Furthermore, increasing interference with PLIN2 expression alleviated the inhibitory effect of glucose on mitochondrial aerobic respiration, while overexpressing PLIN2 directly inhibited mitochondrial aerobic respiration. Therefore, PLIN2, as a key protein regulating mitochondrial aerobic respiration, mediates the oxidation and utilization of fatty acids in renal tubular epithelial cells, promoting the progression of diabetic tubular injury and renal function decline in DKD, acting both as a marker and a regulatory factor.

It is worth noting that overexpression of PLIN2 can activate the PPARγ signaling pathway and inhibit podocyte apoptosis in DKD [30], suggesting that PLIN2 may play different roles in DKD. Knockout of PLIN2 increases the expression of PPARα and PPARγ coactivator 1α [31]. On the other hand, PPARγ and PPARα promote the expression of PLIN2 at the transcriptional level [32-35]. In different metabolic conditions and cell types, various genetic modifiers regulate PLIN2 expression and post-translational modifications, including genes that control lipid metabolism and those involved in ubiquitination, transcription, and mitochondrial function [36]. PLIN2 regulates lipid hydrolysis, which is beneficial for muscle cells to moderately store lipids and utilize glucose oxidation instead of FAO for energy production [31]. This role is also crucial for the pluripotency of embryonic stem cells, as degradation of PLIN2 often leads to lipidome remodeling, particularly the decrease in cardiolipin and phosphatidylethanolamine, resulting in mitochondrial cristae defects and impaired FAO, which in turn reduces acetyl-CoA and histone acetylation [37]. In neutrophils, PLIN2 accelerates lipid droplet degradation by binding to PPARγ as it migrates from the nucleus to the cytoplasm [38]. PLIN2 also regulates the size of lipid droplets and the changes in neutral lipid composition in liver cells under fasting conditions [39]. Therefore, the expression of PLIN2 is closely related to PPAR, but how PLIN2 regulates renal tubular epithelial cell damage caused by DKD, such as promoting lipid droplet accumulation and inhibiting mitochondrial aerobic respiration, remains unclear. Whether PPAR plays an important role in PLIN2 regulation of DKD progression still requires further investigation.

Detecting PLIN2 in renal tubules will help identify DKD populations at risk for renal function progression and provide a basis for precise intervention. The application value of PLIN2 in predicting DKD-related renal function decline needs to be verified in large cohort studies. The regulatory mechanism by which increased expression of PLIN2 causes lipid droplet accumulation and mitochondrial aerobic respiration impairment in renal tubular epithelial cells is unclear. Furthermore, whether PLIN2 plays a role in the progression of non-diabetic CKD remains to be elucidated.

5. Conclusion

In conclusion, PLIN2 in renal tubules can serve as a new approach for predicting renal function decline in DKD. The increased expression of PLIN2 affects mitochondrial aerobic respiration, mediating lipid droplet accumulation in renal tubular epithelial cells induced by glucose, thereby promoting the progression of DKD.

Funding

Supported by the National Natural Science Foundation of China (No.82270760) and the Natural Science Foundation of Jiangsu Province (No. BK20201497).

Disclosure statement

The authors declare no conflict of interest.

References

[1] Yang W, Luo Y, Yang S, et al., 2018, Ectopic Lipid Accumulation: Potential Role in Tubular Injury and Inflammation in Diabetic Kidney Disease. Clin Sci (Lond), 132(22): 2407–2422. https://doi.org/10.1042/CS20180702

[2] Jun H, Song Z, Chen W, et al., 2009, *In Vivo* and *In Vitro* Effects of SREBP-1 on Diabetic Renal Tubular Lipid Accumulation and RNAi-Mediated Gene Silencing Study. Histochem Cell Biol, 131(3): 327–345. https://doi.org/10.1007/s00418-008-0528-2

[3] Falkevall A, Mehlem A, Palombo I, et al., 2017, Reducing VEGF-B Signaling Ameliorates Renal Lipotoxicity and Protects against Diabetic Kidney Disease. Cell Metab, 25(3): 713–726. https://doi.org/10.1016/j.cmet.2017.01.004

[4] Yoshioka K, Hirakawa Y, Kurano M, et al., 2022, Lysophosphatidylcholine Mediates Fast Decline in Kidney Function in Diabetic Kidney Disease. Kidney Int, 101(3): 510–526. https://doi.org/10.1016/j.kint.2021.10.039

[5] Tervaert TW, Mooyaart AL, Amann K, et al., 2010, Pathologic Classification of Diabetic Nephropathy. J Am Soc Nephrol, 21(4): 556–563. https://doi.org/10.1681/ASN.2010010010

[6] Terryn S, Jouret F, Vandenabeele F, et al., 2007, A Primary Culture of Mouse Proximal Tubular Cells, Established on Collagen-Coated Membranes. Am J Physiol Renal Physiol, 293(2): F476–F485. https://doi.org/10.1152/ajprenal.00363.2006

[7] Johansen KL, Chertow GM, Foley RN, et al., 2021, US Renal Data System 2020 Annual Data Report: Epidemiology of Kidney Disease in the United States. Am J Kidney Dis, 77(4 Suppl 1): A7–A8. https://doi.org/10.1053/j.ajkd.2021.01.002

[8] Glastras SJ, Pollock CA, 2024, Targeted Identification of Risk and Treatment of Diabetic Kidney Disease. Nat Rev Nephrol, 20(2): 75–76. https://doi.org/10.1038/s41581-023-00796-9

[9] Oshima M, Shimizu M, Yamanouchi M, et al., 2021, Trajectories of Kidney Function in Diabetes: A Clinicopathological Update. Nat Rev Nephrol, 17(11): 740–750. https://doi.org/10.1038/s41581-021-00462-y

[10] Yamanouchi M, Skupien J, Niewczas MA, et al., 2017, Improved Clinical Trial Enrollment Criterion to Identify Patients with Diabetes at Risk of End-Stage Renal Disease. Kidney Int, 92(1): 258–266. https://doi.org/10.1016/j.kint.2017.02.010

[11] Coca SG, Nadkarni GN, Huang Y, et al., 2017, Plasma Biomarkers and Kidney Function Decline in Early and Established Diabetic Kidney Disease. J Am Soc Nephrol, 28(9): 2786–2793. https://doi.org/10.1681/ASN.2016101101

[12] Wong MG, Perkovic V, Woodward M, et al., 2013, Circulating Bone Morphogenetic Protein-7 and Transforming Growth Factor-β1 are Better Predictors of Renal End Points in Patients with Type 2 Diabetes Mellitus. Kidney Int, 83(2): 278–284. https://doi.org/10.1038/ki.2012.383

[13] Looker HC, Colombo M, Hess S, et al., 2015, Biomarkers of Rapid Chronic Kidney Disease Progression in Type 2 Diabetes. Kidney Int, 88(4): 888–896. https://doi.org/10.1038/ki.2015.199

[14] Mayer G, Heerspink HJ, Aschauer C, et al., 2017, Systems Biology-Derived Biomarkers to Predict Progression of Renal Function Decline in Type 2 Diabetes. Diabetes Care, 40(3): 391–397. https://doi.org/10.2337/dc16-2202

[15] Li KY, Tam CHT, Liu H, et al., 2023, DNA Methylation Markers for Kidney Function and Progression of Diabetic Kidney Disease. Nat Commun, 14(1): 2543. https://doi.org/10.1038/s41467-023-37837-7

[16] Shimizu M, Furuichi K, Toyama T, et al., 2013, Long-Term Outcomes of Japanese Type 2 Diabetic Patients with Biopsy-Proven Diabetic Nephropathy. Diabetes Care, 36(11): 3655–3662. https://doi.org/10.2337/dc13-0298

[17] An Y, Xu F, Le W, et al., 2015, Renal Histologic Changes and the Outcome in Patients with Diabetic Nephropathy. Nephrol Dial Transplant, 30(2): 257–266. https://doi.org/10.1093/ndt/gfu250

[18] Mohandes S, Doke T, Hu H, et al., 2023, Molecular Pathways that Drive Diabetic Kidney Disease. J Clin Invest, 133(4): e165654. https://doi.org/10.1172/JCI165654

[19] Liu H, Doke T, Guo D, et al., 2022, Epigenomic and Transcriptomic Analyses Define Core Cell Types, Genes and Targetable Mechanisms for Kidney Disease. Nat Genet, 54(7): 950–962. https://doi.org/10.1038/s41588-022-01097-w

[20] Doke T, Susztak K, 2022, The Multifaceted Role of Kidney Tubule Mitochondrial Dysfunction in Kidney Disease Development. Trends Cell Biol, 32(10): 841–853. https://doi.org/10.1016/j.tcb.2022.03.012

[21] Vallon V, Thomson SC, 2020, The Tubular Hypothesis of Nephron Filtration and Diabetic Kidney Disease. Nat Rev Nephrol, 16(6): 317–336. https://doi.org/10.1038/s41581-020-0256-y

[22] Kang HM, Ahn SH, Choi P, et al., 2015, Defective Fatty Acid Oxidation in Renal Tubular Epithelial Cells has a Key Role in Kidney Fibrosis Development. Nat Med, 21(1): 37–46. https://doi.org/10.1038/nm.3762

[23] Yuan Q, Lv Y, Ding H, et al., 2021, CPT1α Maintains Phenotype of Tubules via Mitochondrial Respiration During Kidney Injury and Repair. Cell Death Dis, 12(8): 792. https://doi.org/10.1038/s41419-021-04085-w

[24] Feng L, Gu C, Li Y, et al., 2017, High Glucose Promotes CD36 Expression by Upregulating Peroxisome Proliferator-Activated Receptor γ Levels to Exacerbate Lipid Deposition in Renal Tubular Cells. Biomed Res Int, 2017: 1414070. https://doi.org/10.1155/2017/1414070

[25] Itabe H, Yamaguchi T, Nimura S, et al., 2017, Perilipins: A Diversity of Intracellular Lipid Droplet Proteins. Lipids Health Dis, 16(1): 83. https://doi.org/10.1186/s12944-017-0473-y

[26] Li H, Dixon EE, Wu H, et al., 2022, Comprehensive Single-Cell Transcriptional Profiling Defines Shared and Unique Epithelial Injury Responses During Kidney Fibrosis. Cell Metab, 34(12): 1977–1998.e9. https://doi.org/10.1016/j.cmet.2022.09.026

[27] Yang L, Jiang S, Zhang R, et al., 2022, Rab18 Down-Regulates PLIN2 Through the JAK2/STAT3 Pathway and Attenuates Lipid Accumulation in THP-1 Macrophages. Chin J Pathophysiol, 38(5): 769–778.

[28] Jiang S, Zhang R, Li XG, et al., 2021, PLIN2 Promotes Lipid Accumulation in RAW264.7 Macrophages by Regulating SREBP2. Chin J Pathophysiol, 37(1): 1–9.

[29] Blot G, Karadayi R, Przegralek L, et al., 2023, Perilipin 2-Positive Mononuclear Phagocytes Accumulate in the Diabetic

Retina and Promote PPARγ-Dependent Vasodegeneration. J Clin Invest, 133(19): e161348. https://doi.org/10.1172/JCI161348

[30] Dai ZW, Cai KD, Xu LC, et al., 2020, Perilipin2 Inhibits Diabetic Nephropathy-Induced Podocyte Apoptosis by Activating the PPARγ Signaling Pathway. Mol Cell Probes, 53: 101584. https://doi.org/10.1016/j.mcp.2020.101584

[31] Feng YZ, Lund J, Li Y, et al., 2017, Loss of Perilipin 2 in Cultured Myotubes Enhances Lipolysis and Redirects the Metabolic Energy Balance from Glucose Oxidation Towards Fatty Acid Oxidation. J Lipid Res, 58(11): 2147–2161. https://doi.org/10.1194/jlr.M079764

[32] Zhang Y, Fu J, Li C, et al., 2023, Omentin-1 Induces Mechanically Activated Fibroblasts Lipogenic Differentiation Through pkm2/yap/pparγ Pathway to Promote Lung Fibrosis Resolution. Cell Mol Life Sci, 80(10): 308. https://doi.org/10.1007/s00018-023-04961-y

[33] Stojanović O, Altirriba J, Rigo D, et al., 2021, Dietary Excess Regulates Absorption and Surface of Gut Epithelium Through Intestinal PPARα. Nat Commun, 12(1): 7031. https://doi.org/10.1038/s41467-021-27133-7

[34] Pawella LM, Hashani M, Eiteneuer E, et al., 2014, Perilipin Discerns Chronic from Acute Hepatocellular Steatosis. J Hepatol, 60(3): 633–642. https://doi.org/10.1016/j.jhep.2013.11.007

[35] Ke Q, Xiao Y, Liu D, et al., 2024, PPARα/δ Dual Agonist H11 Alleviates Diabetic Kidney Injury by Improving the Metabolic Disorders of Tubular Epithelial Cells. Biochem Pharmacol, 222: 116076. https://doi.org/10.1016/j.bcp.2024.116076

[36] Roberts MA, Deol KK, Mathiowetz AJ, et al., 2023, Parallel CRISPR-Cas9 Screens Identify Mechanisms of PLIN2 and Lipid Droplet Regulation. Dev Cell, 58(18): 1782–1800.e10. https://doi.org/10.1016/j.devcel.2023.07.001

[37] Wu Y, Chen K, Li L, et al., 2022, Plin2-Mediated Lipid Droplet Mobilization Accelerates Exit from Pluripotency by Lipidomic Remodeling and Histone Acetylation. Cell Death Differ, 29(11): 2316–2331. https://doi.org/10.1038/s41418-022-01018-8

[38] Pu Q, Guo K, Lin P, et al., 2021, Bitter Receptor TAS2R138 Facilitates Lipid Droplet Degradation in Neutrophils During *Pseudomonas aeruginosa* Infection. Signal Transduct Target Ther, 6(1): 210. https://doi.org/10.1038/s41392-021-00602-7

[39] Doncheva AI, Li Y, Khanal P, et al., 2023, Altered Hepatic Lipid Droplet Morphology and Lipid Metabolism in Fasted Plin2-null Mice. J Lipid Res, 64(12): 100461. https://doi.org/10.1016/j.jlr.2023.100461